Emittance Growth in a Low Energy Proton Beam

John A. Palkovic
Superconducting Supercollider Laboratory *
2550 Beckleymeade Avenue
Dallas, TX 75237

Abstract

We have measured emittances in a low energy proton beam at energies between 19 and 45 KeV and currents between 9 and 39 mA. The rms emittance of the space charge dominated proton beam, as measured by a moving-slit emittance probe, grew by an average amount of 60% in a propagation distance of 2.5 cm. An Abel inversion procedure was applied to the measured transverse charge distribution of the proton beam in order to calculate the electrostatic field energy, which is the driving quantity for emittance growth. We have found that all of the emittance growth is due to a halo containing $\simeq$ 10% of the beam particles.

I. INTRODUCTION

This paper is a report on an experimental investigation of space-charge driven emittance growth in a low-energy proton beam. The emittance[1] growth of a space charge dominated beam is given by a differential equation which relates the change of the emittance with z, the axial length coordinate, to changes in the field energy: [1]

$$\frac{d\varepsilon^2}{dz} = -\frac{KX^2}{2}\frac{d}{dz}\left(\frac{U}{W_0}\right), \tag{1}$$

where $U = W - W_u$ and W is given by

$$W = \pi\varepsilon_0 \int_0^\infty rE_r^2 dr\,. \tag{2}$$

Physically, W_u is the electrostatic field energy per unit length of a uniform beam with the same current and energy as the real beam. It is calculated from

$$W_u = W_0\left(1 + 4\ln(b/X)\right),\ b \geq X, \tag{3}$$

where b is the radius of the (assumed present) beam pipe and $X = 2\sqrt{\overline{x^2}}$ is twice the width of the beam. $W_0 = (eN)^2/16\pi\varepsilon_0$ is the field energy within the uniform beam, with the logarithmic term giving the contribution from the field outside of the beam.

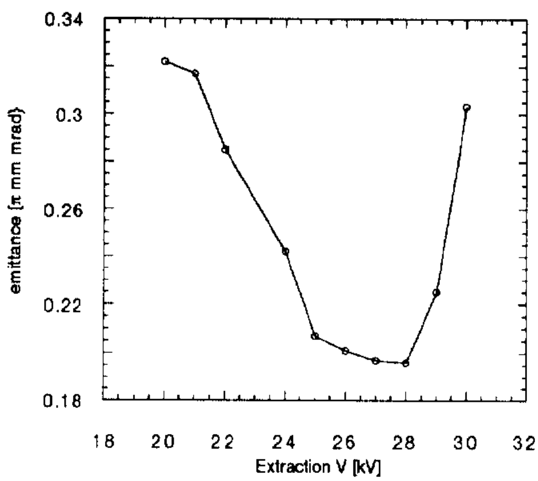

Figure 1. Emittance vs. extraction voltage.

The proton beam was generated by a duoplasmatron which is capable of producing proton currents in excess of 100 mA. However, the peak current in the experiment was limited by the acceptance of the emittance probe to 30 mA or less. The primary diagnostic used in the experiment was the moving slit emittance probe. In addition, a toroidal current transformer and a Faraday cup were used for current measurement.

A set of measurements was done solely on the "young" beam immediately out of the ion source. The emittance seen out of the source depends on many factors — filament current, arc voltage, gas pressure, etc. A reproducible method of generating a beam with a given emittance was needed. It was found that for any setting of the ion source parameters used to produce extracted beam, there was a minimum value of emittance that was obtained as the extraction voltage was varied. This is shown in Fig. 1. The procedure to acquire data that was used for the emittance measurements was to change the ion source arc voltage and the accelerating voltage to produce a desired energy and current, then the extraction voltage was varied until a minimum emittance was found. This ensured that the beam was matched into the accelerating column.

By varying the extraction voltage, the shape of the "plasma emissive meniscus" from which the beam is extracted in the expansion cup of the duoplasmatron is changed. [2] This directly affects the angular distribution of

*Operated by Universities Research Association for the U.S. Department of Energy under Contract No. DE–AC35–89ER40486.

[1] The rms emittance of a beam is given by the formula

$$\varepsilon_x = \frac{4}{p_z}\sqrt{\langle x^2\rangle\langle p_x^2\rangle - \langle xp_x\rangle^2}$$

where p_z is the average momentum of the particles in the direction of motion of the beam; x and p_x are a transverse displacement and momentum, respectively. With an azimuthally symmetric beam, $\varepsilon_x = \varepsilon_y = \varepsilon$.

the emitted beam, as ions tend to leave along trajectories normal to the meniscus. Since the shape of the distribution function $f(x, x')$ is changed, the emittance changes.

II. ABEL INVERSION

As was mentioned above, the emittance growth of a space charge dominated beam is driven by the electrostatic field energy of the beam. Thus we are interested in calculating the electrostatic field energy from the measured distribution function of the beam. A necessary part of this process is the Abel inversion of the density profile. It is easy to extract the distribution $f(x)$ from the measured data. Since the beam is azimuthally symmetric, what is needed is $f(r)$. It is straightforward to calculate the electric field from $f(r)$ by solving Poisson's equation.

A moving-slit emittance probe measures the projection of the six-dimensional beam phase-space onto the transverse "trace-space" $x - x'$. [2] The intensity $I(x)$ of the integrated signal measured at a particular value of x, is given by

$$I(x) = \int_{-\infty}^{+\infty} f(r)dy. \tag{4}$$

Using the fact that x, y, and r are related by the Pythagorean theorem, dy can be expressed in terms of dr to yield

$$I(x) = 2\int_{x}^{+\infty} \frac{rf(r)dr}{\sqrt{r^2 - x^2}}. \tag{5}$$

We say that $I(x)$ is the Abel transform of $f(r)$. This is an integral equation which must now be solved for $f(r)$, the quantity of physical interest. The solution can be written as [3]

$$f(r) = -\frac{1}{\pi}\int_{r}^{\infty} \frac{\left(\frac{dI}{dx}\right)dx}{\sqrt{x^2 - r^2}}. \tag{6}$$

The literature on the numerical evaluation of Eq. (6) is large. This form of the solution is not suitable for application to experimental data, for several reasons. There is a singularity in the integrand, and the evaluation of the derivative dI/dx tends tc introduce large errors, since the intensity $I(x)$ is discretely sampled. Therefore, we would like to express the inverse transform in a different form. Also, real data has a noise component, which can be amplified by the inversion process, particularly for points near the origin. [4] It is desirable to remove the noise with a digital filter while processing the data.

It can be shown that the Fourier, Hankel, and Abel transforms form a set known as the FHA cycle; i.e., applying the Abel transform and then the Fourier transform to a function, we obtain the Hankel transform.[3] The Fourier and Hankel transform can be computed with fast Fourier transform (FFT) algorithms, thus decreasing the computation time required. [5]

We write the Fourier transform of Eq. (4) as

$$\mathcal{F}\{I(x)\} = \int_{-\infty}^{+\infty}\int_{-\infty}^{+\infty} f(r)exp(-i2\pi xq)dxdy \tag{7}$$

Using a standard identity from the theory of Bessel functions, Eq. (7) can be recast as

$$\mathcal{F}\{I(x)\} = 2\pi\int_{0}^{+\infty} rf(r)J_0(2\pi rq)dr \tag{8}$$

The right hand side of Eq. (8) is the Hankel transform of $f(r)$. The inverse Hankel transform is identical to the forward Hankel transform, hence Eq. (7) and (8) lead to

$$f(r) = 2\pi\int_{0}^{+\infty} qJ_0(2\pi rq)\int_{-\infty}^{+\infty} I(x)exp(-i2\pi xq)dxdq \tag{9}$$

Eq. (9) is the form which was used for the inversion of the experimental data. This result has several advantages over Eq. (6). There is no singularity in the integrand. The data can be filtered in the transform domain to smooth it. [6] Considering the baseband nature of the data, a low pass filter is appropriate. A filter with a bandwidth of 0.2 times the Nyquist frequency was used. This smoothing is an important part of the Abel inversion process. Without smoothing the output would contain noise which is the Abel transform of the input noise. The use of FFT routines increases the speed with which the calculations can be done on a computer, and the absence of the derivative in Eq. (9) removes a source of (numerical) uncertainty in the analysis.

Given the radial distribution function $f(r)$, we wish to calculate the field energy per unit length of the beam W, since that is the driving quantity for emittance growth. The radial electric field is easily calculated from Gauss' law; with the electric field determined, the field energy per unit length can be calculated from Eq. (2).

III. DATA INTERPRETATION

The result of an Abel inversion for a measured beam distribution is shown in Fig.(2). The high frequency noise evident in $I(x)$ is completely gone after Abel inversion to obtain $f(r)$. It has to be remembered that the uncertainty in $f(r)$ is largest near the origin of r when comparing the results of two inversions. [4] Since it is the product r and $f(r)$ which is integrated to obtain $E_r(r)$, the input noise does introduce uncertainty into W. This was born out in the experiments, which showed that W varied by ±5% over a set of 20 runs taken with identical ion source parameter settings.

The two most important quantities observed were the beam emittance and the electrostatic field energy of the beam distribution. We recall that it is the electrostatic field energy that drives the emittance growth. A total of 370 emittance was studied.

One observation that was made concerns the shape of the function $f(r)$. Emittance was measured at three different positions along the beam axis. We shall call them z_1, z_2, and z_3. At position z_1, we observed that the beam had a hollow shape. This is illustrated by the distribution in Fig. 3, which shows the result of the Abel inversion procedure for a single emittance run. This shape can be changed

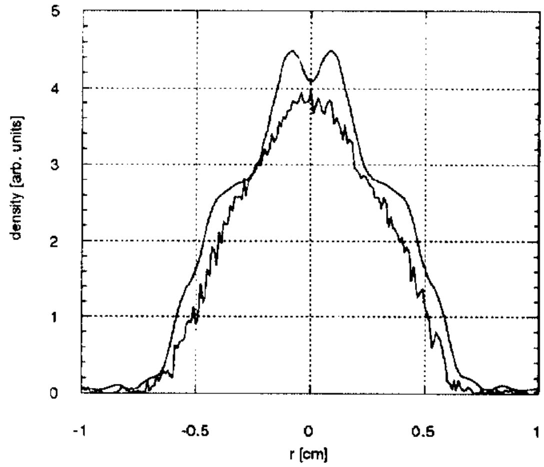

Figure 2. Input x density and inverted density $f(r)$ for 45 keV proton beam. The upper curve is the radial density, which is plotted with negative abscissa values for comparison.

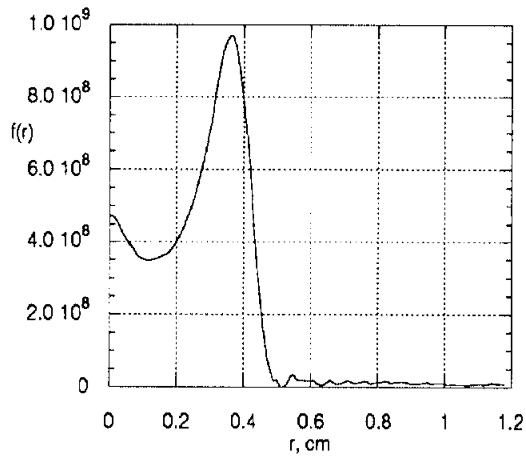

Figure 3. "Hollow" beam distribution from the z_1 position. The ordinate is in cm^{-3}.

somewhat by varying the ion source parameters. However, we found that the hollow shape was predominant at the z_1 position with the extraction optics tuned for minimum emittance as stated above.

When the emittance probe was moved out 5.9 cm to z_2, it was found that the beam was no longer hollow. It had assumed more of a flattened shape, with a "peak" in the middle, as in Fig. 4. As before, the figure corresponds to a single emittance run. Moving another 2.5 cm to position z_3, the beam has assumed an even more pronounced peaked shape in its distribution. This is shown in Fig. 5, which shows a typical beam. The interpretation is that the particles on the edge of the beam at position z_1 have moved into the region near the beam axis due to an inward component of radial velocity. Of course, the space charge of the beam also contributes to development of this shape,

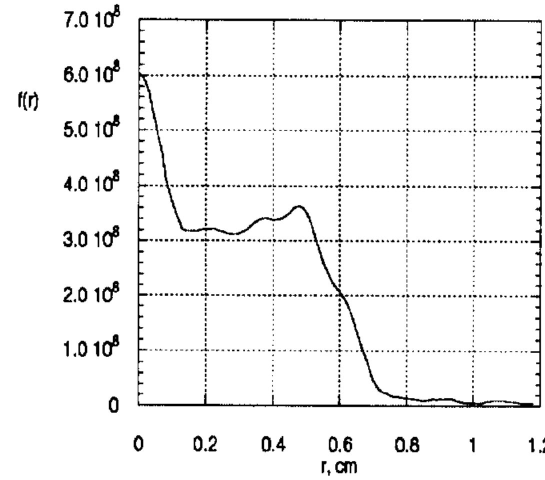

Figure 4. Sample beam distribution at the z_2 position.

although it is not easy to untangle the two contributions.

An important statement of the theory of space charge dominated beams is the equation of energy conservation given by

$$T + W = const. \tag{10}$$

where W is the field energy/unit length of the beam, defined above, and T is given by

$$T = p_z \left\langle x'^2 \right\rangle \left(\frac{I}{q} \right), \tag{11}$$

where $x' = p_x/p_z$. Eq. 11 is derived from a similar result in the literature. [7] Physically, T is the transverse kinetic energy per unit length of the beam. The two quantities T and W were tabulated for each emittance run. We find that the average value of $T+W$, as measured at the three longitudinal positions, is constant within the statistical spread in the data. The results, tabulated from all the data, are shown in Table III..

A correlation was found between the quantity U of Eq. (1) and the rms width of the beam. This is plotted in Fig. (6). This particular correlation was unexpected when first seen. This is perhaps the most striking relationship found in the data. We know of no satisfactory quantitative explanation for it. Qualitatively, the relationship seen is that the smaller beams have more nonlinear field energy. This quantity is strongly dependent on the shape of the distribution function. It is considered to be a property of the duoplasmatron. Although not shown on the graph, the points with the largest U values come mostly from the emittance measurements at position z_1, immediately outside the exit of the ion source.

Perhaps the most dramatic prediction of emittance growth theory is the large "explosive" growth of emittance that a beam experiences when injected into a uniform focusing channel. This growth is predicted to occur in a distance $\lambda_p/4 = m\omega_p/p_z$, where ω_p is the plasma frequency of the beam. [8] Several comments are appropriate before

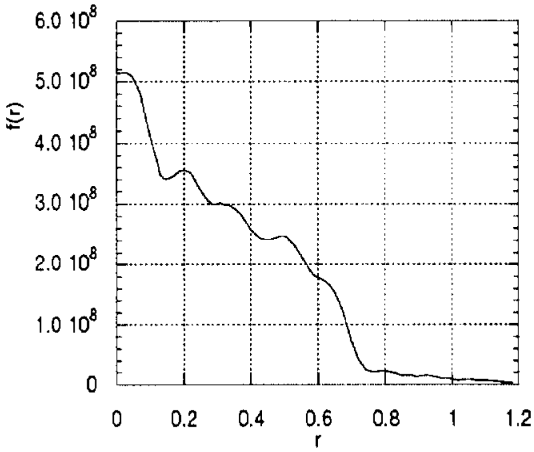

Figure 5. Sample beam distribution at the z_3 position.

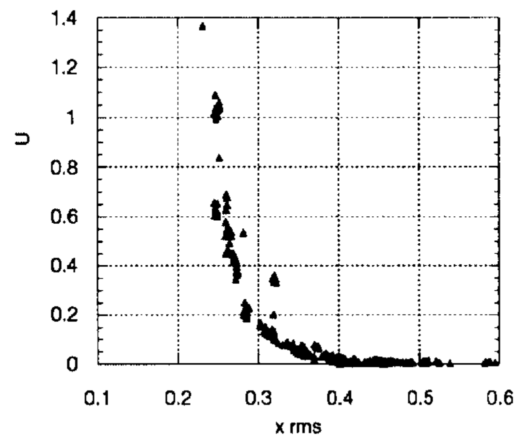

Figure 6. Nonlinear field energy U (dimensionless) vs. rms beam size in cm.

Table 1
Field energy vs. position. T and W are measured in Joules/m.

$T + W$	z,cm
$(2.9 \pm 1.6) \times 10^{-6}$	0.0
$(5.1 \pm 3.2) \times 10^{-6}$	5.9
$(6.5 \pm 3.5) \times 10^{-6}$	8.4

we reach any conclusion on the nature of any such growth in the data presented here.

Rms fitting procedures suffer from a sensitivity to outliers; that is, a small subset of data points that are far from the mean can contribute a large amount to the rms value. In our case, these outliers came from electrical noise on the wires in the backplane of the emittance measuring apparatus. The effect of the noise on the rms emittance calculated from the measured beam data was to make the calculated rms emittance much larger than the true rms emittance of the beam. The outliers introduced by noise could increase the rms emittance by a factor of 2-4. Measurements taken with no beam incident on the probe indicated random noise voltages were present at the $V \leq 0.015$ Volt level. In order to eliminate this spurious contribution to the emittance, a cut was taken at the 0.015 volt level. It was seen that approximately 10% of the wire readings in a typical emittance run contribute to the calculation, the other 90% being noise since little or no beam was incident on these wires.

As was done with the field energy data, it is possible to tabulate the average rms emittances for the three positions at which emittance data was taken. This is shown in Table 1. There is no significant growth in the rms emittance as the beam propagates from z_1 to z_2, a distance of 5.9 cm. As the beam moves from z_2 to z_3, however, the average measured emittance has grown by a factor of 1.6. This certainly qualifies as a large, fast growth.

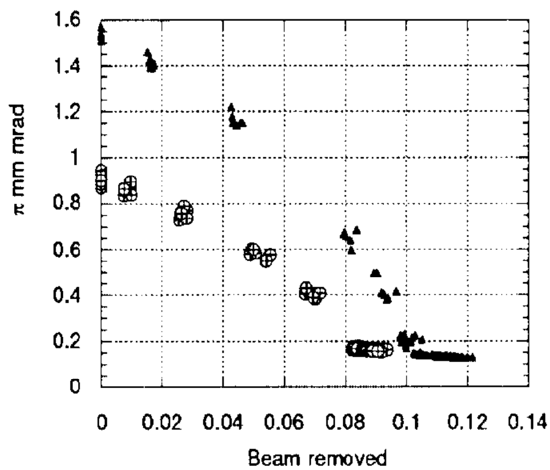

Figure 7. RMS emittance vs. fraction of beam removed.

The typical value of $\lambda_p/4$ for the beams measured was 13.3 cm. Simulations published in the literature often neglect the emittance of the initial beam, and also assume that the beam is subjected to an external force field. In addition, the initial distributions are idealized abstractions which do not completely simulate the charge distribution of a real beam. It is not clear how to relate this observation of emittance growth in a drifting beam to published emittance growth curves. It is plausible that the sharp growth seen is strongly dependent on the initial distribution.

We have found that almost all of the emittance growth is due to particles in the "halo" of the beam, i.e. particles which are positioned near the edge of the distribution in phase space. Fig. (7) is an illustration of this effect. This figure was produced by taking two sets of emittance runs and then increasing the level of the cut from the minimum level (0.015 volts) upward until there was no emittance growth evident at all. Then the fraction of beam removed is calculated. This is proportional to the volume of the

Table 1. RMS Emittance vs. position for low-energy proton beam

ϵ, $\pi mm - mrad$	z, cm
$0.98 \pm .31$	0.0
$1.02 \pm .32$	5.9
$1.60 \pm .15$	8.4

distribution that is removed, i.e. the change in the integral

$$V = \int\int f(x, x')dxdx'. \tag{12}$$

We see that all of the emittance growth is due to the approximately 10% of the beam particles which are in the halo of the beam. In the core of the beam, the curve is flat. In the upper curve, which represents data from position z_3, a larger percentage of the beam has moved into the halo. This contributes significantly to the rms emittance.

IV. CONCLUSION

In conclusion, there has been much excellent theoretical work published in the field of low energy beam transport. We have performed some new measurements to test the most important aspect of the theory of emittance growth in a space charge dominated beam. The results obtained are not inconsistent with the theory. This is not surprising, since it is well founded in classical physics. We have found some new correlations which were not predicted by the theory.

It is a well known fact that emittance grows for almost any beam as it propagates through most any kind of transport line or accelerating structure. The dynamics of this process for a cold space charge dominated beam were predicted to show an explosive growth, and that has been observed. Another important prediction is the constancy of the field energy sum for a drifting beam, $T + W$. This is also verified, although not with high precision. We have found that the emittance growth observed is due entirely to particles in the halo of the beam. If a cut is taken in an emittance run data set which removes 10% of the beam particles, the emittance growth vanishes.

V. ACKNOWLEDGEMENT

The author would like to thank F. Mills and K. Symon for stimulating discussions and for their assistance and guidance in performing this work. This work was performed at Fermi National Accelerator Laboratory, which is operated by Universities Research Association under contract with the U.S. Department of Energy.

VI. REFERENCES

[1] T.P. Wangler., K.R. Crandall, R.S. Mills, and M. Reiser, IEEE Trans. Nucl. Sci. **32**, 2196 (1985).

[2] C. Lejeuene. volume 13 C of *Advances in Electronics and Electron Physics*, pg. 207. Academic Press, 1980.

[3] R.N. Bracewell. *The Fourier Transform and Its Applications.* McGraw-Hill, New York, 1977.

[4] L.M. Smith. *IEEE Transactions on Information Theory*, **34**, 158, 1988.

[5] L.M. Smith. *Journal Quantum Spectroscopy and Radiation Transfer*, **39**, 367, 1988.

[6] J.F. Kaiser and W.A. Reed. *Review of Scientific Instruments*, **48**, 1447, 1977.

[7] I. Hoffman and J. Struckmeier. *Particle Accelerators*, **21**, 69, 1987.

[8] O.A. Anderson. *Particle Accelerators*, **21**,197, 1987.